

A Case Study: Determination of Maximum Spacing of Heat Detectors

SOONIL NAM*

*FM Global Research
1151 Boston-Providence Turnpike
Norwood, MA 02062, USA*

ABSTRACT: The current method of assigning the maximum heat detector spacing based on fire tests that compare detector response to that of a sprinkler does not produce clear performance criteria for detectors. Wide variation in the maximum spacing assigned by testing laboratories for the same type of detectors is another strong indication of the lack of principle behind the concept of testing detectors, and it adds more confusion. Instead, it is proposed in this paper that the maximum detector spacing should be determined based on a specific mission that is expected to be achieved by using detectors. An example introduced in this work shows: (1) how that can be accomplished, and (2) how the spacing determined here makes a lot more engineering sense than that determined by the current method.

KEY WORDS: heat detector response, detector spacing, pre-action system, fire detector, RTI, performance-based detector spacing.

BACKGROUND

CURRENTLY, EACH HEAT detector is characterized by its temperature rating and its maximum spacing. Measuring the temperature rating of a detector is quite straightforward. In general, oven tests are used for the task. The temperature of air circulating inside an oven, to which a detector sample is exposed, is slowly increased until the sample responds. Since there is very little room for any error and the test itself is quite simple, the same results are obtained regardless of the testing laboratory that conducts the measurement.

*E-mail: Soonil.nam@fmglobal.com

The maximum spacing assigned to detectors, however, seldom shows agreements among leading listing organizations. Conceptually, the maximum spacing is the maximum distance from a reference fire that a detector can be positioned while responding either as fast as or faster than a reference detection device installed at a fixed distance from the fire. Currently, an ordinary response sprinkler with a temperature rating of 71°C is used as the reference device in the UL test [1], while a sprinkler with a temperature rating close to the temperature rating of the detector under consideration is used as the reference device in the FM Approvals' test [2]. The reference sprinkler is to be installed at the center of a 3.0 m × 3.0 m spacing. Understandably, the maximum spacing assigned to a detector through these tests can vary widely depending on: (1) test room size, (2) ceiling height, (3) test fire size, (4) test environment, such as ambient temperature and humidity, and (5) temperature rating of the reference sprinkler, among other things.

Not surprisingly, there are large variations in the maximum spacing assigned by UL and FM Approvals for identical detectors. The distances assigned by UL tend to be larger values than those assigned by FM Approvals, mainly because UL conducts the tests in a smaller room than that of FM Approvals while using a larger test fire than that of FM Approvals. It is not uncommon that a detector assigned to a 15-m spacing by UL is given only a 9-m spacing by FM Approvals. In consequence, a detector spacing that is perfectly acceptable to one jurisdiction may not meet the standards of other jurisdictions, depending on the listing requirements of each jurisdiction. The current situation can generate confusion to end users and can create potentially unpleasant issues in certain fire-incident cases.

Even if somehow the tests were standardized to eliminate the confusion surrounding the maximum spacing, still the fundamental question remains. "What does the maximum spacing really mean? Does this guarantee that the detector will respond precisely when it is needed?" No one seems to be able to provide affirmative answers to those questions because the current maximum spacing does not have clear objectives behind it. A more relevant question should be, "What spacing is needed in order for the detector to respond before the fire size becomes larger than X kW?" Detector spacing should be mission specific, and should be determined on a case-by-case basis.

A recent study [3] shows that the response time index (RTI) of heat detectors can be used as a means of assessing heat detectors' thermal response sensitivity to fires. The study also shows how the RTI can be measured and how the measured RTI values can be utilized to calculate detector response times, provided that either the heat release rate (HRR) of a fire with respect to time is known or can be estimated. Thus, the RTI values

assigned to detectors would enable the questions raised above to be answered. By discussing a problem that was encountered recently, this paper intends to show how the maximum spacing of a detector should be determined.

DESCRIPTION OF THE PROBLEM AND THE PROCESSES TO GET THE SOLUTION

The details of the problem to be resolved were as follows:

A warehouse, which stores 5.8-m-high-heavy-weight-roll-paper stacks under a 11.6-m high ceiling, is protected by a dry-pipe system equipped with a preaction valve that is to be tripped by a heat detector. It was requested to determine the largest allowable detector spacing without compromising the full advantage of the preaction system. The main advantage of a detector-tripped preaction dry-pipe system over an ordinary dry-pipe system is that the preaction system is tripped by a detector well in advance of sprinkler actuation, so that the system can be ready to discharge water as soon as sprinklers open.

A sketch of the feed-main piping system is given in Figure 1 and a sketch of the dry-pipe branch pipe system is given in Figure 2. As shown in Figure 2, the system consisted of two sets of separate branch lines. The nominal diameter of the branch pipes is 32 mm (1.25 inch) and that of the two cross mains is 76 mm (3 inch). Six sprinklers are attached at each branch pipe, 3.53 m apart from each other. The distance between the branch pipes is 2.03 m. Thus, the sprinkler spacing is 3.53 m × 2.03 m. The total volume occupied by compressed air, which is the entire volume shown in Figure 2 including the riser, is approximately 1.03 m³. The supervisory air pressure of the system is 129 kPa (4 psig). The design static water pressure just below

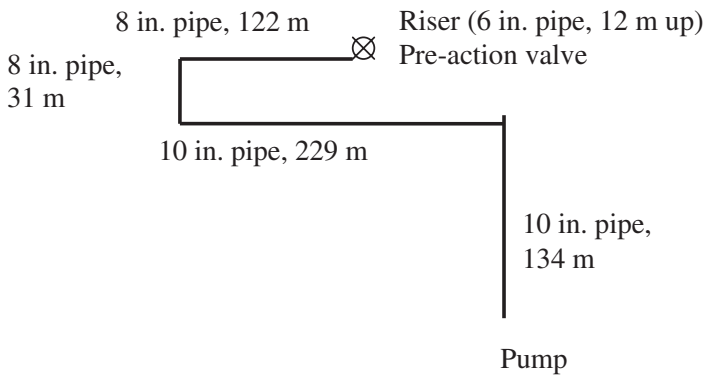


Figure 1. Sketch of the feed-main pipe section of the dry-pipe sprinkler system.

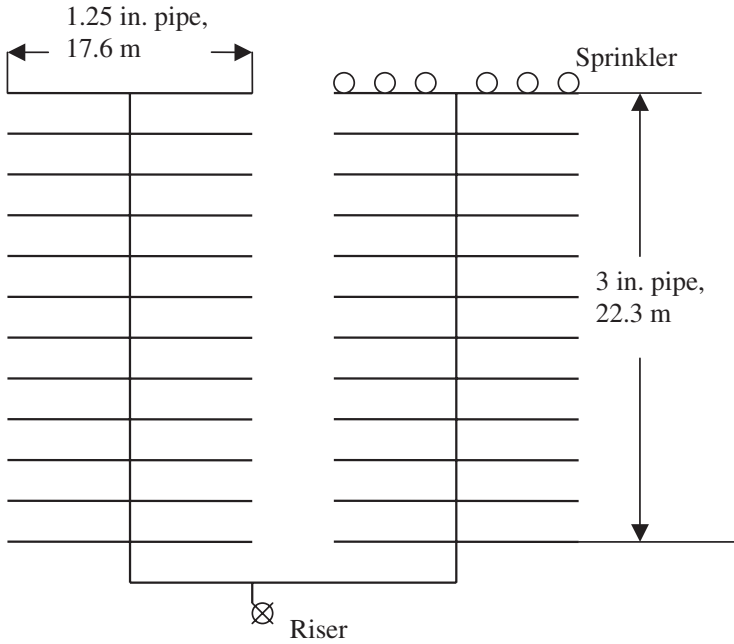


Figure 2. Sketch of the branch lines of the dry-pipe system.

the riser is 894 kPa (115 psig). Thus, under the most ideal situation, approximately 86% of the dry-air volume can be occupied by water before a sprinkler actuates once the preaction valve is tripped. A preaction system cannot be fully equivalent to a corresponding wet system. The system cannot be filled with 100% water before a sprinkler actuates because the air inside the system will be compressed so that the air and water pressures match. Furthermore, if the actuated sprinklers happened to be located where the compressed air pocket is, then air must be discharged first before any water comes out through the open sprinklers. If these concerns can be set aside, piping with 86% of its volume filled with water before sprinkler actuation is the best one can expect from the given system.

In order to take advantage of the preaction system, its valve must trip well before a sprinkler actuates so that the maximum allowable volume of the system can be filled with water at sprinkler actuation. Thus, the time difference between the response of a heat detector that trips the preaction valve and the actuation of the first sprinkler must be larger than the time required for the water to fill 86% of the system volume, provided that the time required to open the valve completely is negligible. It is, therefore, necessary to find out the response times of the detector and the sprinkler,

and the time required for water to fill the system. The following steps will show how those values were obtained.

Water Filling Time

The time required for water to fill 86% of the dry-pipe volume was computed by using a computer program [4] to calculate the “water delay times” in dry-pipe systems (this computer program and reference [4] are proprietary, but a commercially available code [5] can be used for the calculation). In order to calculate the time required to fill 86% of the dry-pipe system with water, details of the piping system, dry-pipe air pressure, and the relation between water flow rates and the water pump pressures must be provided to the program.

The pump performance curve shows that the pump pressures were linear to $\dot{Q}_w^{1.85}$, where \dot{Q}_w is the water flow rate in gpm and pressure is in psig. Table 1 shows a few reference points between the water flow rate and the pump pressure.

The computation showed that the time required would be 17 s. Thus, the detector must respond at least 17 s earlier than the first sprinkler actuates.

Sprinkler Actuation Time

The temperature rating of the sprinklers installed on the ceiling of the warehouse is 141°C. The RTI of the sprinklers is 234 (m s)^{1/2}. The sprinkler response time with negligible conduction effects can be computed by solving the following equation [6]:

$$\frac{dT_e}{dt} = \frac{u^{1/2}}{RTI} (T_g - T_e), \quad (1)$$

where T_e is the sprinkler heat-sensing element temperature, t is the time, u is the ceiling flow velocity surrounding the sprinkler, and T_g is the surrounding

Table 1. Pump pressures versus water flow rates.

Water flow rate	Pump pressure
0 m ³ /s	970 kPa (126 psig)
5.68 × 10 ⁻² m ³ /s (900 gpm)	929 kPa (120 psig)
8.20 × 10 ⁻² m ³ /s (1300 gpm)	888 kPa (114 psig)
1.10 × 10 ⁻¹ m ³ /s (1740 gpm)	757 kPa (95 psig)

hot-air temperature. In order to solve the above equation, the data of u and T_g with respect to time are needed.

One of the most conservative fire scenarios regarding a preaction system is that a fire is located directly under a sprinkler, which happens to be at the center of the detector spacing – therefore the most remote location from the surrounding heat detectors. Thus, the sprinkler can actuate at the earliest possible time, while the heat detector would respond at the latest possible time and trip the preaction valve at the latest possible moment. Following the above scenario, the sprinkler is assumed to be located at the fire plume center axis where the elevation is the same as the ceiling clearance.

The following plume correlations [7] can be used to estimate the centerline temperature and velocity of the plume at the ceiling, if the convective portion of HRR, \dot{q}_c , is known

$$\Delta T_0 = 9.1 \left[\frac{T_\infty}{g C_p^2 \rho_\infty^2} \right]^{1/3} \dot{q}_c^{2/3} (z - z_0)^{-5/3}, \quad (2)$$

$$V_{z_0} = 3.4 \left[\frac{g}{C_p \rho_\infty T_\infty} \right]^{1/3} \dot{q}_c^{1/3} (z - z_0)^{-1/3}, \quad (3)$$

where ΔT_0 (K) is the excess temperature at the plume centerline, T_∞ (K) is the ambient temperature, g (m/s^2) is the gravitational acceleration, C_p (kJ/kg K) is the constant pressure specific heat of air, ρ_∞ (kg/m^3) is the density of ambient air, \dot{q}_c (kW) is the convective component of the HRR, z (m) is the elevation of interest (e.g., the ceiling) in the plume, z_0 is the elevation of the virtual origin of the plume, and V_{z_0} (m/s) is the axial plume centerline velocity. In the following discussion, the quantity “ $z - z_0$ ” is regarded as the elevation above the top surface of the burning fuel array (i.e., the ceiling clearance above the burning fuel in this case).

In order to solve Equations (2) and (3), the HRR of burning 5.8-m-high-heavy-paper-roll stacks, which are stored in the warehouse, must be found or estimated. Because actual HRR data from this fuel array were not available, the HRR had to be estimated as follows. Historical records related to fire tests that used 5.8-m-high-newsprint-roll-paper stacks as a fuel under a 9.1-m high ceiling were located. It was found that the plume axis temperature at the ceiling height in these records could be expressed as

$$\Delta T_0 = 57(t - 24), \quad (4)$$

where t is the time in seconds. Then \dot{q}_c can be obtained by converting Equation (2) to the following equation:

$$\dot{q}_c = 9.1^{-3/2} \left(\frac{g}{T_\infty} \right)^{1/2} C_p \rho_\infty (z - z_0)^{5/2} \Delta T_0^{3/2}, \quad (5)$$

Inserting Equation (4) into (5) yields

$$\dot{q}_c = 70\tau^{3/2}, \quad (6)$$

where \dot{q}_c is in kW, $\tau \equiv t - 24$, and z_0/z is assumed to be negligible.

Now that \dot{q}_c is known, Equations (2) and (3) will provide u and T_g at the elevation of the ceiling above the top surface of the burning fuel array ($z = 11.6 \text{ m} - 5.8 \text{ m} = 5.8 \text{ m}$) for Equation (1), and then a proper numerical integration until T_e becomes the sprinkler rating temperature will yield the time of sprinkler actuation. A computational program using a fourth-order Runge-Kutta scheme was used to show that the sprinkler would actuate when $t = 50 \text{ s}$ for an ambient temperature of 20°C .

Detector Response Times

A sample of the same type of detector, shown in Figure 3, currently installed at the warehouse was subjected to the plunge test described in reference [3]. The test results indicated that the RTI of the detector was $14 \text{ (m s)}^{1/2}$. The temperature rating of the detector is 57°C . Since the RTI value and the temperature rating of the detector are known, the response time of the detector can be calculated with high precision using Equation (1), as shown in [3], once the temperature and the velocity of a fire plume at the detector location are known.

The computations were carried out for two cases of the maximum detector spacings, $15.2 \text{ m} \times 15.2 \text{ m}$ and $7.6 \text{ m} \times 7.6 \text{ m}$. Following the fire scenario, the detector was assumed to be located at the center of either the $15.2 \text{ m} \times 15.2 \text{ m}$ spacing or the $7.6 \text{ m} \times 7.6 \text{ m}$ spacing; thus, the detector, which was mounted on the ceiling, was located at either 10.7 or 5.4 m radial distance from the fire plume axis. In order to estimate the fire plume velocities and the temperatures at the detector locations, correlations that show the velocities and the temperatures as a function of a radial distance r from a plume centerline must be known, preferably in functional forms.

Although there are many ceiling flow correlations, new correlations were devised in this work mainly because: (1) the degree of scatter of the data

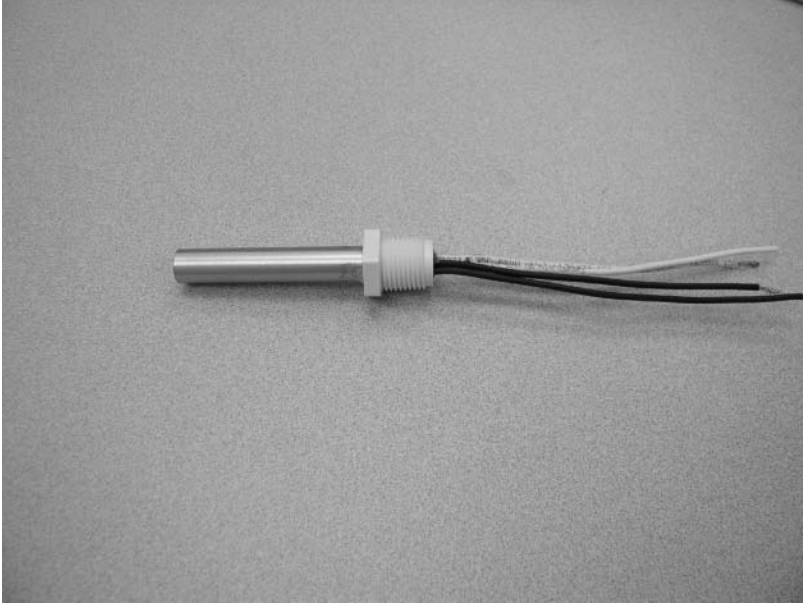


Figure 3. The heat detector currently installed at the warehouse that is the example of the analysis in this work.

associated with the correlations could be seen on one hand, and (2) many sets of data on ceiling flows were readily available on the other hand. For anyone who does not want to go through the development of custom correlations, reference [8] provides a list of existing ceiling jet flow correlations.

Figure 4 shows data of $\Delta T(r)$, the excess ceiling flow temperature at location r , normalized by ΔT_0 , which is the excess temperature on the axis of an unobstructed fire plume at the elevation corresponding to the ceiling height. The radial distance, r , was normalized by b , which is the half-width of an unobstructed fire plume at the elevation corresponding to the ceiling height. The plume half-width can be calculated [7] as follows:

$$b = 0.12 \left(\frac{T_0}{T_\infty} \right)^{1/2} (z - z_0), \quad (7)$$

where T_0 is $\Delta T_0 + T_\infty$.

The data in the figure include the work of Pickard et al. [9], Thomas [10], Heskestad and Hamada [11], and the author. Pickard et al. measured the ceiling flows generated by alcohol pan fires, the diameters of which ranged

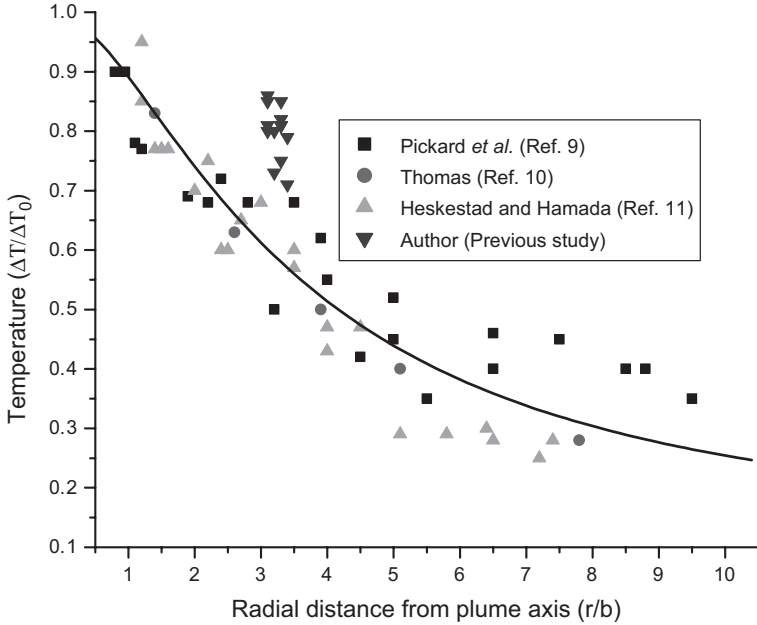


Figure 4. Ceiling flow data of temperature vs. radial distance and a correlation curve.

from 0.15 to 0.9 m (HRR varied between 4.85 and 128 kW) under the ceiling heights ranging from 1.2 to 2.4 m. Thomas used 0.42 m diameter alcohol pan fires (HRR = 106 kW) under a 1.37-m high ceiling. Heskestad and Hamada used propane burners, the diameters of which varied from 0.15 to 0.61 m (HRR varied between 11.6 and 382 kW) under the ceiling heights ranging from 0.56 to 2.5 m.

The author, in a previous study, used heptane *spray* fires ranging from 400 to 613 kW. The flow rate of the heptane sprays during the tests was from 13.13 to 19.95 ml/s. Spray nozzles were placed 1.2 m above the floor under a 5.8-m high ceiling; thus, the ceiling clearance above the nozzles was 4.6 m. The temperatures and the velocities of the ceiling jets were measured by thermocouples and bidirectional velocity probes installed 0.15 m below the ceiling at a 2.2-m radial distance from the fire source axis. As the fire plume from spray fires inherits momentum associated with sprays from nozzles, the temperatures and velocities from the data obtained by the author were expected to be slightly higher than the corresponding temperatures and velocities from the other data sets, which were obtained from purely buoyant fire plumes. The data from Pickard et al. and Thomas were converted to fit the normalizations as shown in the figure. A correlation was

developed based on the data and is shown in the figure. The functional form is

$$y = y_0 + \left[\frac{a}{(w\sqrt{\pi/2})} \right] \exp \left\{ -2 \left[\frac{(x - x_c)}{w} \right]^2 \right\}, \quad (8)$$

where $y \equiv \log(\Delta T/\Delta T_0)$, $y_0 = -0.00781$, $a = -1.2788$, $w = 1.23898$, $x \equiv \log(r/b)$, and $x_c = 1.51005$.

Figure 5 shows a collection of data showing V_r/V_{z_0} versus (r/b) . V_r is the radial directional flow velocity at r and V_{z_0} is the centerline axial velocity of an unobstructed fire plume at the elevation corresponding to the ceiling height.

The data of Kung *et al.* [12] in the figure are a collection of nine, 3-minute fire tests burning two- to four-tier rack storage of commodity (see [12]) consisting of double tri-wall cartons with metal liners on a wood pallet, under a 9.1-m high ceiling. The ceiling clearances during the tests

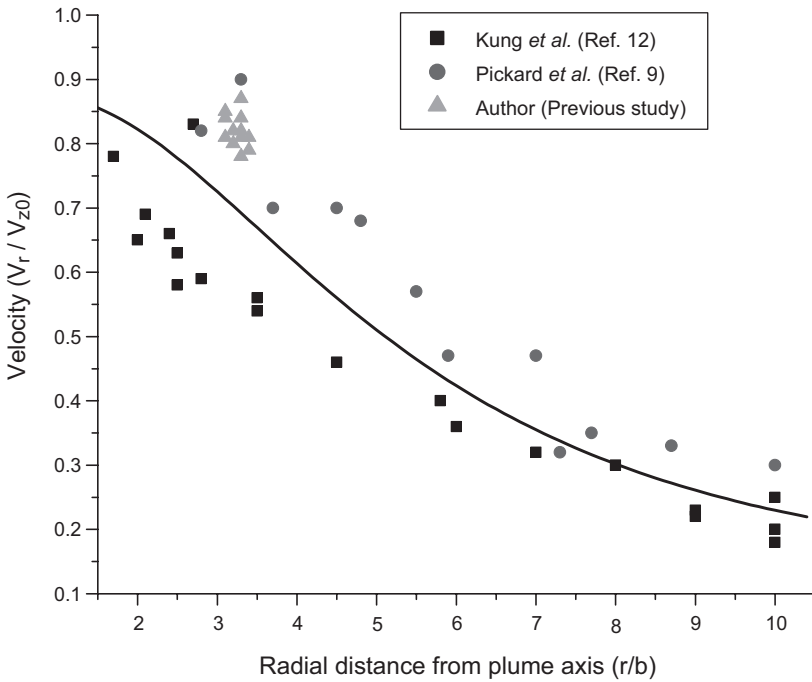


Figure 5. Ceiling flow data of radial velocity vs. radial distance and a correlation curve.

Table 2. Response times of the sprinkler and the detectors.

Ambient temperature (°C)	Response time (s)		
	Sprinkler directly above fire	Detector (7.6 × 7.6 m ² spacing)	Detector (15.2 × 15.2 m ² spacing)
-7	55	35	42
-1	54	34	41
4	53	34	40
10	52	33	38
16	51	32	37
21	50	31	36
27	50	30	35

varied from 1.3 to 5.9 m and the estimated maximum HRR of each test varied from 8.4 to 14 MW. A correlation curve is given in the figure, the functional form of which is the same as Equation (8), however, with different values of the parameters. Here $y \equiv \log(V_r/V_{z_0})$, $y_0 = -0.5514$, $a = -0.79891$, $w = 0.79131$, and $x_c = 1.31777$. Now all the data necessary to carry out the computations are collected. The temperature and velocity variations with time at $r = 5.4$ or 10.7 m can be obtained by applying Equation (2) through (8). Then Equation (1) can be numerically integrated until T_c reaches the detector-rating temperature, 57°C . Table 2 shows the response times of the sprinkler, the detector located at $r = 5.4$ m, which corresponds to the $7.6 \text{ m} \times 7.6 \text{ m}$ spacing, and the detector located at $r = 10.7$ m, which corresponds to the $15.2 \text{ m} \times 15.2 \text{ m}$ spacing, under various ambient temperatures.

Table 2 shows that the time difference between the response of the sprinkler and the response of the detector installed with the $7.6 \text{ m} \times 7.6 \text{ m}$ spacing is about 19 s. It is larger than the time required for water to fill up the system, which is 17 s. Thus, the detectors installed with the $7.6 \text{ m} \times 7.6 \text{ m}$ spacing are likely to provide a timely response to open the preaction valve and in turn it would provide the maximum advantage of the preaction dry-pipe system. The time difference between the response of the sprinkler and the response of the detector installed with the $15.2 \text{ m} \times 15.2 \text{ m}$ spacing, however, is about 13 s, which is shorter than the time required for water to fill up the system. In consequence, the detector spacing of $15.2 \text{ m} \times 15.2 \text{ m}$ is not likely to allow the system to take its full advantage. The calculation, therefore, indicates that the warehouse in this example should use the $7.6 \text{ m} \times 7.6 \text{ m}$ as its maximum detector spacing rather than the $15.2 \text{ m} \times 15.2 \text{ m}$ spacing.

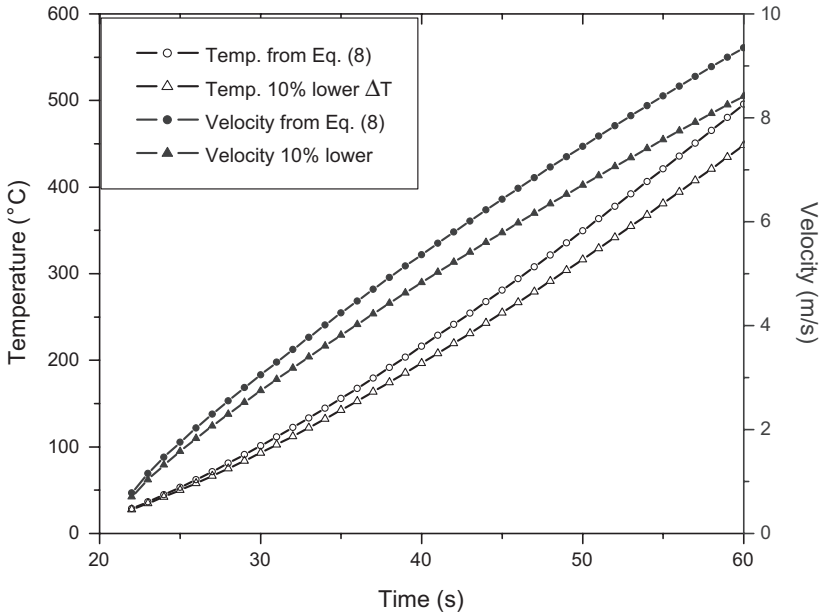


Figure 6. Ceiling flow temperature and velocity from Equation (8) at the detector in the $7.6\text{ m} \times 7.6\text{ m}$ spacing and the temperature and the velocity corresponding to 10% lower ΔT and V , than those from Equation (8).

Whenever an engineer makes this kind of prediction, all the uncertainties associated with the engineering correlations, the experimental data, and the final computational results should be carefully weighed.

For instance, in order to assess the impact associated with the uncertainties in the ceiling flow temperatures and velocities expressed by Equation (8), detector activation times were recalculated by using excess temperatures and velocities that are 10% lower than those obtained from the correlations (excess temperatures and velocities higher than those from the correlations need not be considered – see below). The ceiling flow temperatures and the velocities at the detector in the $7.6\text{ m} \times 7.6\text{ m}$ spacing are obtained from Equation (8) and are shown in Figure 6. Compared with the values in Table 2, the detector at the center of the $7.6\text{ m} \times 7.6\text{ m}$ spacing took: (1) one second longer than the response times in Table 2 when both the ceiling flow excess temperatures and velocities were 10% lower than the corresponding values used in the table, (2) one second longer than the response times in Table 2 when the ceiling flow excess temperatures were 10% lower than, but the velocities were unchanged from, the corresponding values used in the table, and (3) the same response times in Table 2 when the ceiling flow velocities were 10% lower than, but the excess temperatures

were unchanged from, the corresponding values used in the table. Thus, the ceiling flow correlations within 10% uncertainties did not seem to make any impact on the overall performance expected from the detector in this particular case.

Considering other factors relevant to risk analysis associated with fire scenarios would be helpful too.

CONCLUDING REMARKS

The current maximum heat detector spacing assigned by listing organizations does not seem to provide clear performance criteria. The maximum distances are determined through fire tests, in which the detector samples are spread out at various distances from the source of a fire and the response times are measured. Among the detector samples that respond prior to the response of a reference sprinkler located at a 2.2-m radial distance from the fire source, the distance corresponding to the most remote detector sample becomes the basis for the maximum spacing. Understandably, it is unlikely that someone can tell what the specific engineering significance of this spacing is. In addition, the test results can vary widely depending on test conditions. In consequence, the maximum spacing even for the same type of detectors seldom agrees among the leading testing organizations, which just adds more confusion to end users.

The analysis introduced here shows how the maximum detector spacing was assigned – mission specific and site specific. The example used here is a real case problem that was requested to be solved. The processes used here are quite straightforward and easy to understand, because the decision was made based on a specific engineering problem with a clear objective in mind. The maximum detector spacing in other cases also can be and, perhaps, even *should* be determined following similar processes illustrated in this work – achieving a specific goal from use of detectors.

REFERENCES

1. UL 539, “UL Standard for Safety for Single and Multiple Station Heat Detectors,” 5th ed., Underwriters Laboratories Inc. (UL), 333 Pfingsten Road, Northbrook, Illinois, 2000.
2. “Thermostats for Automatic Fire Detection,” Class Number 3210, FM Approvals, 1151 Boston-Providence Turnpike, Norwood, Massachusetts, 1978.
3. Nam, S., Donovan, L.P. and Kim, G., “Establishing Heat Detectors’ Thermal Sensitivity Index through Bench-Scale Tests,” *Fire Safety Journal*, Vol. 39, 2004, pp. 191–215.
4. Nam, S. and Kung, H.C., “Theoretical Prediction of Water Delay Time of Dry-Pipe Sprinkler Systems in the Event of Fire,” FMRC Technical Report, J. I. 0T0R8.RA, Factory Mutual Research Corporation, Norwood, Massachusetts, 1993.

5. Golinveaux, J., "Calculated Water Delivery Time for Large Dry Pipe Systems," NFPA World Safety Conference & Exposition, Dallas Convention Center, Dallas, Texas, May 18–21, 2003.
6. Heskestad, G. and Bill, R.G., "Quantification of Thermal Responsiveness of Automatic Sprinklers Including Conduction Effects," *Fire Safety Journal*, Vol. 14, 1988, pp. 113–125.
7. Heskestad, G., "Engineering Relations for Fire Plumes," *Fire Safety Journal*, Vol. 7, 1984, pp. 25–32.
8. Alpert, R., "Ceiling Jet Flow," Chapter 2, *The SFPE Handbook of Fire Protection Engineering*, 3rd ed., Society of Fire Protection Engineers, Bethesda, Maryland, 2002.
9. Pickard, R.W., Hird, D. and Nash, P., Note NO. 247, Fire Research Station, Boreham Wood, Herts, 1957.
10. Thomas, P.H., Note No. 141, Note NO. 247, Fire Research Station, Boreham Wood, Herts, 1955.
11. Heskestad, G. and Hamada, T., "Ceiling Flows of Strong Fire Plumes," *Fire Safety Journal*, Vol. 21, 1993, p. 69.
12. Kung, H.C., You, H.Z. and Spaulding, R.D., "Ceiling Flows of Growing Rack Storage Fires," In: 21st Symposium (International) on Combustion, Combustion Institute, Pittsburgh, Pennsylvania, 1986, p. 121.